



## **DESIGN CONSIDERATIONS FOR SHREDDER FEED CONVEYORS USED IN FARM AND FOOD INDUSTRY**

**Andrzej Tomporowski**

*University of Technology and Life Sciences  
ul. Prof. S. Kaliskiego 7, 85-789 Bydgoszcz  
Tel./fax: +48 52 3408255  
e-mail: [a.tomporowski@wp.ptl](mailto:a.tomporowski@wp.ptl)*

### *Abstract*

*The purpose of conveyors, designed depending on the type of raw material and requirements with regard to the comminuted materials is to ensure smooth and efficient comminution procedure. Scientific literature provides detailed descriptions and studies focusing on the functionality and operational characteristics of systems used for feeding long (continuous) materials; corn stems, plastics, branches (wood) and other similar materials. These descriptions usually refer to the design features of shredders in connection with applicable operational characteristics. Nonetheless, despite the existence of various types of conveyors intended for feeding long materials, it is still a pertinent issue to ensure high effectiveness, including consistent feed, and efficiency of the feeding equipment. Based on both own research and the studies by other academics, it has been proven that the design of the working units applied in the analysed equipment, aside from the properties of the fed material and the applicable process parameters, has a significant influence on consistent and efficient energy consumption.*

### **1. Introduction**

The production and processing of specific materials used in the farm and food industry depend largely on the development of modern engineering and technological solutions. The key element in the production and processing of this type of materials is the process generally referred to as comminution of raw and base materials used in the farm and food industry.

Primary processing of these materials develops equally dynamically as engineering solutions focused on the management and recovery of waste from these materials. Comminution is an essential stage of each production and subsequent recirculation process, both in the initial as well as the final phase of a full cycle. The purpose of conveyors, designed depending on the type of raw material and requirements with regard to the comminuted materials is to ensure smooth and efficient comminution procedure. Scientific literature provides detailed descriptions and studies focusing on the functionality and operational characteristics of systems used for feeding long (continuous) materials; corn stems, plastics, branches (wood) and other similar materials. These descriptions usually refer to the design features of shredders in connection with applicable operational characteristics. Nonetheless, despite the existence of various types of conveyors intended for feeding long materials, it is still a pertinent issue to ensure high effectiveness, including consistent feed, and efficiency of the feeding equipment. Based on both own research and the studies by other academics, it has been proven that the design of the working units applied

in the analysed equipment, aside from the properties of the fed material and the applicable process parameters, has a significant influence on consistent and efficient energy consumption [1,2,4,5].

**The purpose of this study** was to systematize models which support of designing roll feeders for long, continuous materials intended for use in farm and food industry. The study was conducted based on a prototypical shredding unit provided by Jamox company.

## 2. Roll feeder design principles

Roll feeders are commonly utilized in comminution equipment used for shredding continuous (long and fibrous) materials. Porous, continuous materials which, when leaving the roller gap, are much more compacted, displaced and deformed, due to external forces, than the originally fed material, are transferred into the working gap of the feeder.

The process of compacting continuous material within the inter-roll area may be divided into two stages (Fig.1): drawing stage and compacting stage.

By analogy to raw material in the form of uniform and continuous material, it is possible to use existing models based on the principle of continuity, in order to determine relative speed as the difference between the speed of the raw material  $v_s$  and the peripheral speed of the feeding roll surface  $v_r$ :

$$v = v_s - v_r, \quad (1)$$

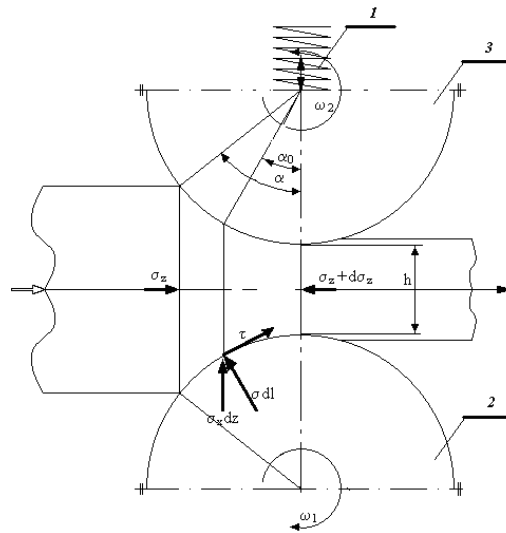


Fig. 1. Functional diagram of a roll feeder; 1) pressure spring, 2) fixed roll, 3) pressure roll

When the material is fed into the inter-roll area the peripheral speed on the surface of the feeding rolls is larger than the linear speed of the raw material. Thus, the relative speed  $v_{rel}$  compared to the roll surface is the smallest and is bound to increase due to the locally decreasing height of the gap  $h(z)$ . The state of balance for an average stress  $\sigma$  and friction angle  $\varphi_w$  between the material and roll surface is defined by the following relationship:

$$h(z) \frac{d\sigma_z}{dz} + 2\sigma_z \operatorname{tg} \alpha = 2\sigma_x \operatorname{tg} (\alpha + \varphi_w) \quad (2)$$

Therefore:

$$\frac{d\sigma_z}{dz} + f(z)\sigma_z(z) + g(z) = 0 \quad (3)$$

From the moment the material is captured by the rolls the surface pressure increases from zero to the maximum value occurring at the point where the relative speed  $v = 0$ . According to these assumptions, this is where the maximum pressure may be observed. The following stages may be identified during spatial compaction of continuous material within the working area of a roll feeder [5]:

1. Initial volume reduction, mutual displacement of individual units of the raw material.
2. Further volume reduction caused by elastic deformations and plastic strains.
3. Burnishing, breaking and fracturing of the fed material.

The first stresses occur within the inter-roll area, in the slip zone. Individual constituents of the raw material meant for comminution come into contact with one another and the fibres begin touching the surface of the walls and rolls. This phenomenon may be described using the principles of mechanics. If the shearing stresses of the wall are sufficient for the given raw material to be drawn without any slip, that point signifies the beginning of an adhesion zone. This is where the material is further compacted, depending on the geometrical conditions. The properties of the continuous material are a reliable basis with regard to the stress pattern.

The stresses occurring within the slip zone are substantially influenced by the pressures generated on the material feeding plane, since these pressure values determine the shearing stresses acting on the walls, towards the roll gap. The higher the pressure of the rolls on the material fed on the roll grip plane  $z_G$  is, the higher the resulting stress with suitably stronger compacted material. The total pressure force may be derived from the integral of the roll perimeter pressure curve.

### 3. Design guidelines

Figure 2 shows the slip zone and adhesion zone in the inter-roll gap. The roll surface exhibits certain lead/advance above the roll grip angle  $\theta_G$  due to as yet insignificant friction stress. The so-called slip state occurs in this area. Below the roll grip angle, the nonslip material drawing causes a certain compaction, correspondingly to the geometrical conditions within the inter-roll gap. At the  $\alpha = 0$  point, the compressed material leaves the roll gap without elastic deformation.

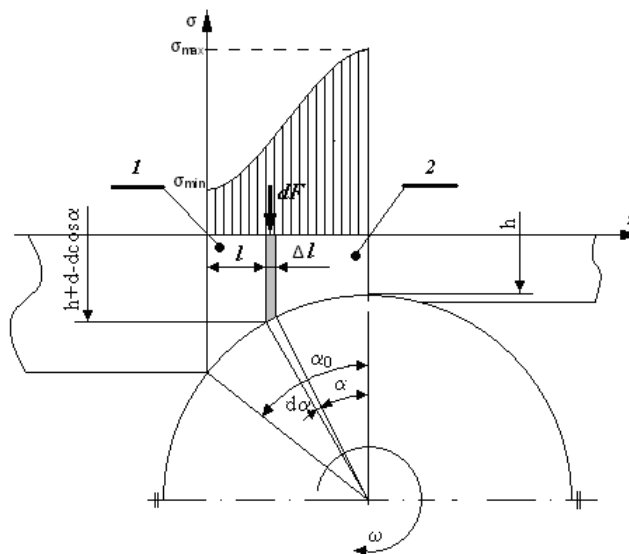


Fig. 2. Slip zone and adhesion zone within a roll area; 1- slip zone, 2- adhesion zone

The analysis of the stress pattern within the working area of the roll feeder (in the roll gap) involves determining:

1. stresses within the slip zone,
2. stresses within the adhesion zone,
3. roll grip angle  $\alpha_G$ .

#### 4. Stresses within the slip zone

The following consideration are based on the assumption that the slip processes, occurring between individual constituents of the fed material and between the fed material itself and the walls of the feeder, are decisive within this area. The material behaviour may be characterized based on, e.g. the effective slip point or the point of slip on the mouth and roll wall. The state of stress within an element of the fed material is described assuming a coexistence of the main stress directions and main deformation directions (unit elongations) with material isotropy acc. Mohr's circle of stresses.

Shear and normal stresses for a given plane are represented as points on the circle of stresses. This way of representation enables determination of stresses on various planes of the analysed fed material volume. Relationships between normal stresses  $\sigma_x$  and  $\sigma_z$  and relatively identical shear stresses  $\tau_{xz}$  and  $\tau_{zx}$  are following:

$$\left\{ \begin{array}{l} \sigma_x = \frac{\sigma_1(1 + \cos \beta) + \sigma_2(1 - \cos \beta)}{2} \\ \sigma_z = \frac{\sigma_1(1 - \cos \beta) + \sigma_2(1 + \cos \beta)}{2} \\ \tau_{xz} = \frac{\sigma_1 \sin \beta - \sigma_2 \sin \beta}{2} \\ \tau_{zx} = \frac{\sigma_1 \sin \beta - \sigma_2 \sin \beta}{2} = \tau_{xz} \end{array} \right. \quad (4)$$

The largest principal stresses  $\sigma_1$  are exerted, in accordance with definition, on the plane free of shear stresses and are turned by a  $\beta/2$  angle in a mathematically negative direction in relation to the direction of normal stress  $\sigma_x$ .

Both stresses on the  $\sigma$  -  $\tau$  plane form a  $\beta$  angle in a mathematically positive direction, while the stresses  $\sigma_x$  and  $\sigma_z$ , as well as  $\sigma_1$  and  $\sigma_2$  form a right angle. That is why the line connecting these stresses on the  $\sigma$  -  $\tau$  plane runs straight through the central point of the Mohr's circle of stresses.

The notion of relative slip between elements of the fed material is understood as plastic strain of its element subject to pressure generated by the feeder rolls. By applying the criterion of inter-material slip, based on the theory of Mohr's circle of stresses, it is possible to determine the plane on which this displacement between the constituents of the fed material occurs, including the related maximum shear stress of this plane.

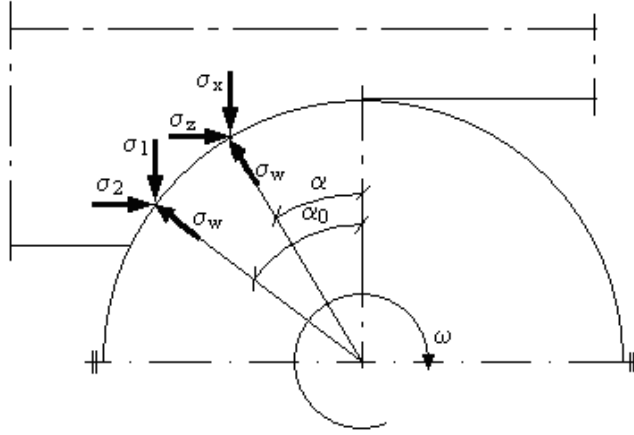


Fig. 3 The stresses that occur on the feeder roll surface

Figure 3 shows the states of stress for two continuous elements of the fed material on the surface of the roll. The elements of the fed material are in a state of elasto-plastic balance with a slip in its volume and on the wall of the feeder mouth. The largest principal stress  $\sigma_1$  forms an angle  $\alpha$  with direction  $x$ , while the stress  $\sigma_w$  forms an angle  $\alpha$  with the negative direction  $x$ . The sum of angles  $\beta + \alpha$  is always present between the stresses  $\sigma_1$  and  $\sigma_w$  on the  $\sigma$ - $\tau$  plane.

Since:  $x = 0$ ,  $\beta = 0$  on the symmetry plane as well, the direction of principal stresses has been established along the whole plane  $z = \text{const}$ , defined by  $\alpha_0$ . On this plane lies the beginning of the coordinate system applied herein. Therefore:

$$\alpha_0 = \frac{1}{2} \left[ \varphi_\omega + \arcsin \frac{\sin \varphi_\omega}{\sin \varphi_e} \right] \quad (5)$$

This plane is referred to as the material feeding plane.

$$\omega = \alpha_0 - \alpha \quad (6)$$

It enables, with identified properties of flow from the coordinate  $\alpha$  determination of direction  $\omega$  of the largest principal strain  $\sigma_1$  on the surfaces of the feeding rolls.

The analysis performed as part of this study did not cover gravitational forces of the fed material exerted on the surface of the bottom feeder roll and the guiding trough. Owing to a relatively small weight and considerably high pressures generated by feeder rolls, these forces were considered irrelevant for the subject matter of this study and were thus omitted. The balance of stresses in the  $z$  and  $x$  direction lead to the following system of equations:

$$\begin{cases} \frac{\partial \sigma_z}{\partial z} + \frac{\partial \tau_{xz}}{\partial x} = 0 \\ \frac{\partial \sigma_x}{\partial x} + \frac{\partial \tau_{zx}}{\partial z} = 0 \end{cases} \quad (7)$$

Therefore:

$$\left\{ \begin{array}{l} (1 + \sin \varphi \cos \beta) \frac{\partial \sigma}{\partial z} - \sin \varphi \sin \beta \frac{\partial \frac{\beta}{2}}{\partial z} + \sin \varphi \cos \beta \frac{\partial \sigma}{\partial x} + \sin \varphi \sin \beta \frac{\partial \frac{\beta}{2}}{\partial x} = 0 \\ (1 + \sin \varphi \cos \beta) \frac{\partial \sigma}{\partial x} + 2\sigma \sin \varphi \cos \beta \frac{\partial \frac{\beta}{2}}{\partial x} + \sin \varphi \sin \beta \frac{\partial \sigma}{\partial z} + 2\sigma \sin \varphi \cos \beta \frac{\partial \frac{\beta}{2}}{\partial z} = 0 \end{array} \right. \quad (8)$$

The increase of stresses in the symmetry axis of the roll gap was identified as an approximate solution, by the application of the integral calculus average value theorem, and it amounts to:

$$\frac{1}{\sigma} \frac{d\sigma}{dz} = \frac{8\alpha_0 - 8\alpha g \varphi_e}{\left[ \frac{s}{2} + \frac{d}{2}(1 - \cos \alpha) \right] \left[ \operatorname{tg} \left( \frac{\alpha_u - \alpha}{2} - \frac{\varphi_c}{2} + \frac{\pi}{4} \right) - \operatorname{tg} \left( \frac{\alpha_u - \alpha}{2} + \frac{\varphi_c}{2} - \frac{\pi}{4} \right) \right]} \quad (9)$$

$$\text{where:} \quad z = \frac{d}{2} \cos(\alpha) \quad (10)$$

therefore, the stresses amount to:

$$\sigma = \sigma_0 \exp \int_0^\alpha f(z) dz \quad (11)$$

## 5. Stresses within the adhesion zone of the feeder

The postulated compression of the fed material in a roll feeder of shredder takes place within the adhesion zone where there are no slips on the smooth surface of the roll. The stress pattern was established based on the volume reduction value in the inter-roll gap of the feeder (Fig. 2). The volume of material in the mouth of the feeder amounts to:

$$V_\theta = [(h + d(1 - \cos \alpha)) \cos \alpha - H] b \Delta l, \quad (12)$$

calculated for width of the rolls which equals  $b$ . The teeth that help drawing the material onto the surface of the rolls were included by introduction of the  $H$  value which stands for an averaged reduction of the substitute gap, which is connected with the volume of a single tooth  $V_R$  and the number of these teeth  $n_R$ , determined by the following equation:

$$\pi d b \frac{H}{2} = n_R V_R \quad (13)$$

The decrease in volume, derived based on the roll grip angle  $\alpha_G$ , results in an increase in compressed material density  $\rho_K$ . The density ratio is as follows:

$$\frac{\rho k_1 \alpha}{\rho k_1 \alpha_G} = \frac{V_{\alpha_G}}{V_\alpha} = \frac{H + (h + d(1 - \cos \alpha_G)) \cos \alpha_G}{H + (h + d(1 - \cos \alpha)) \cos \alpha} \quad (14)$$

The following approximate relationship occurs between density and compressive stress:

$$\sigma \approx \rho_K^k \quad (15)$$

stress pattern in the adhesion zone:

$$\sigma_{\alpha} = \sigma_{\alpha_G} \left[ \frac{H + (h + d(1 - \cos \alpha_G)) \cos \alpha_G}{H + (H + d(1 - \cos \alpha)) \cos \alpha} \right]^K \quad (16)$$

The roll grip angle was derived based on the above equation, therefore:

$$\left. \frac{d\sigma}{dz} \right|_{\alpha} = K\sigma_{\theta} \left[ \frac{d(2 \cos \alpha - 1) - s}{H + [h + d(1 - \cos \alpha) \cos \alpha]} \right] \frac{2tg \alpha}{d} \quad (17)$$

where:

$$\alpha = \arcsin \frac{2(h_0 - z)}{d} \quad (18)$$

## 6. Determination of the feeder roll grip angle

The equation (17) contains the output stress on the  $z = 0$  plane as boundary condition. Based on both stress gradients in the adhesion zone and slip zone, it is possible to determine the feeder roll grip angle. The compaction is conditional upon continuity in the inter-roll gap of the feeder and results in smaller increase in surface pressure due to the compaction that has already occurred. Equal stress gradients are therefore necessary prerequisite for the unknown roll grip angle.

$$\left. \frac{d\sigma_1}{ds} \right|_{\alpha_G} = \left. \frac{d\sigma_2}{ds} \right|_{\alpha_G} \quad (19)$$

The largest principal stress for the roll grip angle amounts to:

$$\sigma_1 = \sigma + \sigma \sin \varphi_e \quad (20)$$

## 7. Pressure and driving power forces

In accordance with figure 2, the pressure force  $F$  was determined by integration of the field below the curve of the surface pressures occurring in the roll gap:

$$F = \frac{bd}{2} \int \sigma_1 \cos \alpha d\alpha \quad (21)$$

Depending on the pressure force, only the surface pressures occurring in the adhesion zone are taken into consideration. The pressures in the slip zone are negligibly low.

$$F = \frac{bd\sigma}{2} \int_0^{\alpha} \left( \frac{h + H}{H[h + d \cos \alpha - d \cos^2 \alpha]} \right) \cos \alpha d\alpha \quad (22)$$

where the maximum stress at the narrowest point of the roll gap amounts to  $\sigma_{1 \max}$ .

The torque was determined through integration of the pressure force on the roll surface in the adhesion zone:

$$M = 0,25Fdtg \alpha \quad (23)$$

The driving power was derived from the relationship between torque and roll revolutions  $n_r$ .

$$P = 2\pi Mn_r \quad (24)$$

## 8. Conclusions

The phenomena, processes and relationships between feeding continuous materials such as tree branches or plant stems and multi-edge grinding are relatively easy to describe formally, despite their complexity and multifaceted nature. Arriving at the answer to the question about process factors (actions and methods), design features (means, devices and systems), operational conditions pertaining to roll feeders and their influence on the dynamics and efficiency of the whole comminution process (tree branches), with a multi-edge shredder used as an example, was possible with an assumption that quasi-cutting stresses will propagate at an infinite rate [3,4,5].

It seems appropriate to continue the research focusing on optimising the design features of the analysed prototypical shredding unit.

*I would like to thank the owners of Jamox Company for making the prototype and required technical resources available for the purpose of this study.*

## References

- [1] Flizikowski, J., *Konstrukcja rozdrabniaczy żywności*, Wydawnictwo Uczelniane Akademii Techniczno – Rolniczej w Bydgoszczy, Bydgoszcz 2005.
- [2] Flizikowski, J., Bieliński, M., *Rozdrabniacz wielotarczowy zwłaszcza do materiałów ziarnistych*, Patent RP.
- [3] Mroziński, A., *Modelling of waste-paper stock treatment process in disc refiners*, Journal of POLISH CIMAC nr 3/2010, Vol. 5, str. 113-119.
- [4] Tomporowski, A., *Testing thy power of multi - disc shrebing grains of rice*, Ekologia i Technika nr 3, s. 161-164.
- [5] Tomporowski, A., *Nierównomierność obciążeń przy rozdrabnianiu drewna*, Recykulacja, Bydgoszcz 2008.